Experimental Behaviour of CFRP Strap Strengthened RC Beams Subjected to Sustained Loads

Experimental Behaviour of CFRP Strap Strengthened RC Beams Subjected to Sustained Loads

Feifei JIN [1], Janet M. LEES[2*]

[1] Former Research Associate, Department of Engineering, University of Cambridge, Cambridge CB2 1PZ, UK

[2] Professor of Civil Engineering, Department of Engineering, University of Cambridge, Cambridge CB2 1PZ, UK

***** Author to whom correspondence should be addressed; e-mail: jml2@eng.cam.ac.uk; Tel.: +44 1223 332678.

Abstract:

Reinforced concrete (RC) beams strengthened with transverse pre-stressed unbonded carbon-fiber-reinforced polymer (CFRP) straps have shown substantial increases in shear capacity when subjected to short-term static loading. However, understanding the time-dependent behaviour is a further prerequisite in order to better evaluate this strengthening technique and its engineering applications. This paper presents time-dependent experimental results from an un-strengthened RC beam and four RC beams strengthened with CFRP straps. The parameters under consideration included the concrete strength, applied load level and pre-stress level in the CFRP straps. The beams were subjected to sustained loads that were fixed percentages of the short-term failure load. To investigate the development of the external concrete strains, the internal steel shear link strains, the strap strains and the shear crack patterns, the beams were monitored over a period of around 320 days. The long-term beam deformations were also recorded and decomposed into bending and shear components. When compared with an equivalent unstrengthened beam, the presence of the CFRP straps reduced the proportion of the shear deflection. However, in the strengthened beams the shear proportions of the total mid-span deflection were still 24% to 28%, which were not negligible. An analysis using a Mohr's circle of strain confirmed that the long-term tensile behaviour in the shear span appears to dominate the development of the shear deformation.

Keywords

Carbon-fiber-reinforced polymer; Shear; Reinforced concrete beams; Sustained load; FRP strengthening, Unbonded prestressed straps

Introduction

Reinforced concrete (RC) beams typically exhibit one of two global failure modes: flexural failures or shear failures. Shear failures can occur suddenly without advance warning, therefore it is important to prevent this type of failure. Several factors can adversely affect the true shear capacity of existing RC beams, such as the corrosion of the internal steel shear links, over-loading, less conservative initial designs and construction defects (Lees et al., 2002). Once an existing structure has been identified as having insufficient shear capacity, the strengthening of RC beams is usually preferable to re-construction (Teng et al., 2002). Since the 1990s, the feasibility of using fiber-reinforced polymers (FRPs) to enhance the flexural strength of RC beams has been extensively researched and validated (e.g. Meier and Kaiser, 1991; Teng et al., 2003; El-Hacha et al., 2003). However, to date, research on shear strengthening has been more limited and the strengthened shear behavior of concrete is not well understood (Lima and Barros, 2011).

A number of fiber-reinforced polymer shear strengthening techniques have been proposed including the use of the epoxy bonded sheets (e.g., Triantafillou, 1998) and near surface mounted reinforcement (e.g., De Lorenzis and Nanni, 2001). However, with an externally bonded system there is the potential for de-bonding failures to occur and the effectiveness of the FRPs cannot be fully exploited when only the accessible regions in the web of the shear span are strengthened. Moreover, research has indicated that the high strain capacity of FRPs can be better utilised when the materials are pre-stressed (e.g. Lees and Burgoyne, 1999; Burgoyne and Balafas, 2007). An innovative shear strengthening technique using pre-stressed

carbon-fiber-reinforced polymer (CFRP) straps (shown schematically in Fig. 1) was first developed by Winistörfer and Meier (Winistörfer, 1999). To form a typical strap, a thin thermoplastic CFRP tape is wrapped around the cross-section of a beam multiple times and the two outermost tape layers are fusion bonded to form an outer closed loop. In this technique, the inner tape layers are not laminated and the CFRP strap is not bonded to the concrete therefore de-bonding issues can be avoided. Another advantage is that the high strength of CFRP material is more efficiently utilised when the strap is pre-stressed.

Experimental studies have been undertaken on the use of pre-stressed CFRP straps to strengthen reinforced concrete columns (Motavalli et al (2010)), to provide additional transverse reinforcement to beams (e.g. Stenger, 2001; Kesse and Lees, 2007; Hoult and Lees, 2009; Dirar et al., 2013; Yapa and Lees, 2013) or to enhance the punching shear resistance of slabs (Koppitz et al, 2014). An initial feasibility study to investigate the potential for CFRP straps to strengthen box girder bridges has also been conducted (Czaderski et al, 2008).

For reinforced concrete beam applications, different aspects of the strengthening system have been studied such as the influence of the CFRP strap spacing, number of strap layers, pre-stress level in the strap, and the optimum design configuration. However, with the exception of two T-beams tested by Hoult and Lees (2011) (one for cyclical loading and the other for sustained loading), the experiments to date have been conducted on beams subjected to short-term loads until failure. Hoult and Lees (2011) conducted a creep experiment on a 3 m long strengthened T-beam subjected to a sustained load equivalent to 80% of the strengthened ultimate capacity for 260 days and found that the shear deflection could be a relatively significant proportion of the total deflection. An increase in the strains in the CFRP straps was also noted and attributed to the concrete creep effects in the shear span.

The general long-term performance of CFRP strengthened RC beams requires further investigation. Particular knowledge gaps include: whether a time-dependent shear failure

could occur when a strengthened beam is subjected to long-term load; and whether there are situations where a CFRP strap with a high initial prestress could reach the ultimate strap failure strain over the long term. These issues will be influenced by the time-dependent shear crack development, concrete shear strain evolution and proportion of the shear deflection in CFRP strengthened beams. A related fundamental factor is the identification of the source of time-dependency in reinforced concrete in shear. This has important ramifications for the in-service behavior of unstrengthened and FRP-strengthened beams more generally.

A series of experiments were designed to better understand the long-term shear behaviour of CFRP strengthened beams and gain a greater insight into the long-term safety of the system. The level of applied sustained load is linked to the imposed stress, the concrete properties relate to the level of concrete creep and the strap preforce dictates not only the vertical precompression applied to the concrete but also the residual strain capacity of the strap. Hence the long-term applied load level, the concrete strength and the percentage of strap prestress were selected to be the most influential parameters in an initial investigation of long-term effects and consequences. A comprehensive measurement scheme to extract pertinent values related to crack and deformation metrics related to the shear behaviour was an important part of the experimental programme. The tests are also valuable in expanding the experimental database for this strengthening technique as well as providing evidence for the calibration and development of time-dependent analytical and numerical material and structural models.

Experimental Programme

An un-strengthened control beam and four beams strengthened with two CFRP straps in each shear span were tested. The beams were subjected to sustained loads under four-point bending. The experimental beams and associated test parameters are summarised in Table 1.

A notation based on BL#/C##/P##/S## was defined where the first grouping indicated the beam specimen, the second denoted the target concrete strength, the third related to the presence of straps and prestress level and the final grouping referred to the sustained load level. Beam BL3/C50/P25/S75 had a target compressive cube strength of 50 MPa whereas a 30 MPa mix was specified for the other beams. In beam BL5/C30/P50/S75 the initial prestress was 50% of the strap failure stress whereas for the strengthened beams BL2-BL4 it was fixed at 25%. The level of sustained load was based on results from short-term failure tests conducted on unstrengthened and strengthened beams with equivalent material and strap configurations as BL1-BL5. For further details please see Jin, 2016. The required sustained load was then fixed as a percentage of the baseline short-term static failure loads. For BL4/C30/P25/S50, this was set at 50% of the shear capacity of the equivalent short-term beam and for the other beams it was set at 75%.

Beam details and reinforcement layout

All beams had identical internal reinforcement as shown in Fig. 2. The overall beam length was 2600 mm. The flexural tensile reinforcement ratio was 3.3% which was sufficiently high to avoid a flexural failure. The shear links consisted of 4 mm diameter smooth steel bars with a spacing of 200mm. In the strengthened specimens, two 10-layer pre-stressed CFRP straps were located at distances of 300 and 500 mm from the beam supports to obtain a high level of shear strength enhancement.

Material properties and CFRP strap prestress

Two different concrete mixes were used. The first mix was designed with a target 28 day concrete compressive cube strength of 30 MPa whereas the second mix had a target strength of 50 MPa. The mix proportions are summarised in Table 2. Three concrete control cubes (100×100×100 mm) were tested on the same day as each beam was loaded and the average compressive cube strength f_{cu} results are presented in Table 1. Beams BL1, BL2, BL3 and BL5

had the same mix proportions but the cube strength of BL5 (32.23 MPa) was slightly higher than BL1-BL3 (25.54-27.83 MPa). Although the added water had been adjusted to reflect the measured moisture content of an aggregate sample it is postulated that the moisture could nevertheless vary within the bulk aggregate material and may have led to a certain variation in water/cement ratio and hence strength between castings. Based on experimental tensile tests on lengths of steel reinforcement, the mechanical properties of the 4-mm, 8-mm, and 16-mm diameter bars are summarised in Table 3. The CFRP straps were formed from a 10 loops of continuous 12mm wide by 0.16mm thick non-laminated CFRP tape consisting of unidirectional CFRP fibers embedded in a thermoplastic resin. The straps were supported on bespoke steel pads on the top and bottom of the beam. As discussed, the target level of initial prestress was either 25% of 50% of the strap ultimate capacity and the prestress was inferred from strain gauges bonded to the outer surface of the strap. Since the prestress was locked in by inserting thin steel shims under one of the steel support pads which was lifted using a hydraulic jack, it was necessary to over-stress the straps during the installation stage to allow for the insertion of the shims. This process was somewhat difficult to control and led to variations in the initial strap prestress. The modulus of elasticity of each strap was approximately 120 GPa with an ultimate strain of 1.3%.

Measurement scheme

Figure 3 presents a schematic overview of the measurement scheme. A total of seven dial indicators were installed underneath the beams to measure the global vertical beam deflections. Square elements were formed on the concrete surface using demec points to track the section-by-section deformation longitudinally along the shear span. The notation for the square elements on the un-strengthened and strengthened beams is shown in Fig 3(a). Each element consisted of four demec points with a 200 mm side length. The stated accuracy of the demec gauge reader for this gauge length was 0.0020 mm. The strains of the measured lengths of the

square elements were derived from the demec measurements as shown in Fig. 3(b). To track the local crack propagation, additional rhomboidal elements were generated on the concrete surface. Each element consisted of four demec gauges with a standard two inch (50.8 mm) side length. The stated accuracy of the demec measurement for this gauge length was 0.0013 mm. Note that BL4 was subjected to a lower sustained load level and the shear cracks were not expected to fully develop, therefore in this beam the local crack propagation was not investigated to the same level of detail as in the other beams. A reference demec measurement relative on an invar reference bar supplied by the manufacturer was taken before and after each set of measurements to help ensure that the demec gauge reader was working properly.

To monitor the behaviour of the internal steel shear links, strain gauges were bonded to both legs of all the shear links at locations along the expected plane of the shear crack. For the CFRP straps, the strain gauges were only bonded on a single leg since a fairly consistent strain development in both sides of the unbonded strap has been observed elsewhere (Hoult, 2005). Strain gauges were also bonded to the longitudinal tensile and compressive steel reinforcement at mid-span. The strain gauge locations for the different reinforcing elements are presented in Fig. 2(b)-(c).

Beam tests

All the beams were simply supported. The two concentrated loads were applied symmetrically with a distance between the load points of 800mm. One loading point was fixed horizontally. The other loading point and the two supports were rollers that allowed free horizontal movement and rotation. All the loading and bearing plates had dimensions of 100mm×100mm×25mm.

The rigs for the time-dependent tests are shown in Fig. 4. Two 30mm diameter threaded steel rods were calibrated to determine the tensile force-strain relationship of the rods, and then

screwed into the strong floor. By tightening the top nuts, a tension force was generated in the rods that reacted against a transverse spreader beam. The load was then transferred to a longitudinal spreader loading beam. The load in the rods was monitored and gradually applied until the target force level was reached. The absolute values of the target loads are summarised in Table 1. To sustain the load over the long term, the nuts needed to be regularly tightened using a wrench attached to a timber lever arm as there was tendency for the load to drop over time due to creep effects.

Initial readings were manually taken from the dial gauge indicators, square demec elements, and equilateral rhomboidal elements. The measurements were then manually repeated on selected dates over the long term.

Results and Discussion

The sustained load was applied for a duration of at least 314 days and readings at either 314 or 320 days were used as a comparator across the five beams. After this period, none of the beams had collapsed. The measured time-dependent shear crack patterns, shear reinforcement strains and beam deformations are presented in the following sections.

Shear crack development

The shear crack patterns on initial loading are presented in Fig. 5. Selected measurements of the crack spacings are also noted. In the un-strengthened control specimen BL1/C30/nS/S75, a single major crack developed in each shear span. However the left span was more critical according to the observed degree of crack opening. The crack tips of the major shear crack in the right span did not reach the support or loading point to the same extent as those in the left span. In the strengthened beams (BL2-BL5), a greater number of shear cracks occurred after initial loading. The inclusion of CFRP straps significantly changed the shear crack pattern and the shear cracks were typically more smeared with uniform spacings.

During the course of the long-term loading, although the crack opening magnitudes of the existing shear cracks increased, no new continuous shear cracks formed. In some of the strengthened specimens, the major shear cracks could not be clearly identified as no single crack dominated. For example, the right shear span of BL2 had an obvious major shear crack but in the left shear span none of the critical cracks could be considered to be critical as the crack openings were much smaller and the crack paths were also shorter. The major shear cracks that intersected one or more strap and tended to separate the shear span were selected for further investigation. These cracks are labelled and the equilateral rhomboidal elements that contained these shear cracks were numbered as shown in Fig. 5. The major shear crack in the left span of BL3 was not investigated as it developed several different branches. Using the measurements from the rhomboidal element, the crack width, w, and crack slip, v, can be calculated according to the geometric relationship before and after concrete cracking as shown in Fig. 3(c).

The resulting crack kinematics along the shear cracks after specific durations are shown in Fig. 6 where the crack width and crack slip are plotted against the element number for beams BL1, BL2, BL3 and BL5. The crack width and slip increased away from the support and typically reached the greatest values in the middle region of the shear crack plane. They then decreased again towards the tip of the crack closest to the loading point. A comparison of the crack width and slip profiles suggests that the maximum crack width and slip did not occur at the same location in the beams and that the propagation depended on the shear crack path. This suggests that the restraint and mixed mode conditions vary along the crack. The slip near the crack tip (elements 10-13) was negligible and the longitudinal steel (near element 1) restrained both the crack width and crack slip. The crack widths were higher than the crack slips but the relationship between these parameters was not constant and varied depending on the location of the element. Consideration of the combined tension and shear stresses along the crack is

therefore necessary to account for these interactions e.g. Foster et al (2015), Foster et al (2017). The magnitude of crack opening increased over the long term, however the shape of the crack kinematics stayed relatively stable. Moreover, the increase in both the crack width and slip depended on the initial magnitudes, which again reinforces the necessity of investigating critical shear cracks.

From a global perspective, although the absolute applied sustained load in BL2/C30/P25/S75 (72 kN) was significantly greater than that in BL1/C30/nS/P75 (38 kN), the crack width and slip in BL2 (right span) were generally lower than in the BL1 (left and right spans). Hence the CFRP straps effectively limited the crack opening development over the long term. The initial crack widths and slips for BL3/C50/P25/S75 were greater than those for BL2/C30/P25/S75. However the time-dependent increases in crack width and slip for BL3 with a measured concrete strength of 46 MPa were less than those for BL2 with a measured strength of 26 MPa. Therefore the higher concrete strength reduced the shear crack opening development over the long term. Although BL5/C30/P50/S75 was subjected to a higher sustained load (83 kN) in an absolute sense than BL2/C30/P25/S75 (72 kN), the crack opening development was broadly similar. This was attributed to differences in the selected major cracks.

Shear reinforcement strains

The time-dependent shear link strains for beams BL1-BL5 are plotted in Fig. 7. The strain gauge readings on the middle shear link of the left shear span of BL1/C30/nS/S75 unfortunately became corrupted after 147 days. The shear crack profiles and crack propagation in the two spans of a given beam differed, so even though the shear link layout was symmetric, the link strains in the left and right spans also differed. The initial formation and propagation of cracks dictate the locations where crack displacements occur thereby generating strain in the transverse reinforcement spanning the cracks. The middle shear links had the highest strains,

which was consistent with the observed crack patterns and measurements. The middle shear links did not yield when the beams were initially loaded but, with the exception of BL4, all the middle links yielded over the long term. The time-dependent strain behaviour depended on the initial magnitude of strain. However, none of the shear links ruptured. A comparison across the strengthened beams shows that the maximum shear link strains were observed in BL3/C50/P25/S75 (R). BL3 was also the beam with the greatest initial crack width (see Fig. 6) thereby providing further evidence of the connection between the link strains and crack profiles.

The CFRP strap strains (excluding the strap pre-strain) are shown in Fig. 8 for BL2-BL5. The percentage strain increases were between 3% and 42% except for the strains in the inner strap in BL4 that decreased by 5%. Again, due to the variable crack patterns, the inner and middle CFRP straps developed different initial strains upon loading. This then had an impact on the strap strain increase over the long term. Hoult (2005) also found that the strap strain increase tended to be a function of the initial strain after loading. This implies that a strap with the highest initial strain (excluding the pre-strain) would typically also experience the greatest strain increase over the long term and this could govern the system integrity. However, the propensity for a strap failure is also related to the initial prestress and hence it is the total strap strain including the pre-strain that is important.

With the exception of BL2, the middle straps had the highest initial and time-dependent strains. None of the straps had ruptured by the end of the long-term loading phase but notable increases in strap strain were observed in some long-term specimens. For example, the maximum percentage strain increase in BL3 was 42% (1715×10^{-6}) and represented around 13% of the full strain capacity of the strap. The highest total strap strain developed in BL5/C30/P50/S75, a beam with straps with a higher initial pre-stress (50%). In this case, the CFRP strain reached 7865×10^{-6} after 314 days. At this strain level some damage to the straps might occur where

small slivers of tape fracture and detach from the strap. Indeed, this phenomenon was observed to some extent during the initial prestressing of the BL5 straps when during the prestressing process, the straps were over-strained to approximately 7000×10^{-6} to allow for the insertion of metal shims under the strap support pads. The fracturing of CFRP slivers at high strap strains has been reported elsewhere (Lees and Winistöerfer, 2010). However, the strap still has a capacity to continue to sustain loads, and this response can be taken as a warning of pending failure. The use of higher initial strap pre-stress more fully exploits the enhancement potential and material utilisation. However a limit on the allowable pre-strain is required in practice to reflect the possible long-term effects and the onset of damage as indicated above.

Time-dependent beam deformation

Shear deformation

For an individual square demec element using the notation shown in Fig. 3, the mean shear strain, γ_{xy}, can be found using equation (1),

$$\gamma_{xy} = 2\varepsilon_{45^o} - \frac{\varepsilon_{x\_top} + \varepsilon_{x\_bottom}}{2} - \frac{\varepsilon_{y\_left} + \varepsilon_{y\_right}}{2} \qquad (1)$$

To investigate the global shear strain in the shear span, the shear strains of each of the three 200 mm square elements were calculated and then averaged. The resulting average shear strains for the left and right spans of the beams are plotted in Fig. 9.

The global shear strains increased by between 141% and 242% after being subjected to sustained loading for approximately 320 days. At that point, the shear strain of the left shear span of the un-strengthened beam BL1/C30/nS/S75was almost twice that of the right shear span. This reflects the dominance of the left span shear crack in BL1. Nevertheless, the percentage increases in the two spans were found to be fairly similar. For the strengthened beams, the inclusion of the CFRP straps reduced the differences between the shear strains in the two spans and the strains in the left and right spans of BL2, BL4 and BL5 were fairly

consistent. Even for BL3 where the biggest differences were noted, the level of difference between the two spans was still much less than in BL1.

A comparison of BL3/C50/P25/S75 and BL2/C30/P25/S75 suggests that the use of higher strength concrete did not significantly reduce the shear strains (both initial and long-term). A contributing factor was that, since the short-term failure load of a BL3 equivalent beam was higher than that of BL2, the absolute value of sustained load on BL3 was also higher leading to higher initial strains. However, even in light of higher initial strains, the percentage increases in the global shear strains were lower for BL3 than BL2. This indicated that the long-term shear strain development was negatively correlated with the concrete strength.

Although the initial strains of BL2/C30/P25/S75 were higher than BL4/C30/P25/S50, the percentage increases in shear strain were fairly similar. So, although the magnitude of long-term shear strain would be expected to be correlated with the magnitude of initial shear strain, the percentage increase did not appear to be affected by the level of external sustained load.

The higher initial prestress level (50%) in the BL5/C30/P50/S75 CFRP straps reduced the percentage increase in the long-term shear strain when compared with BL2/C30/P25/S75 with a strap prestress of 25%. This is also consistent with the role of the CFRP straps in limiting the influence of the concrete creep behaviour.

Investigation of source of time-dependency in shear deformation

For a reinforced concrete element subjected to shear forces, the time-dependency is primarily the result of compressive creep and time-dependent tensile behaviour in the concrete in the two principal directions respectively. The development of the mean shear strain was presented in the previous section but further interrogation is required to determine which mechanism dominates the shear strain increase over the long term. Using a Mohr's circle, the measured strains in the square elements can be converted into components in principal directions as shown in Fig. 10 where compression is defined as a negative strain. As an example, the change

in "R2" (as defined in Fig. 3) is selected and the circles after initial loading and around 320 days are plotted for BL2, BL4 and BL5. The orientations, θ, of the longitudinal strain ε_x and transverse strain ε_y relative to the principal strain directions changed from 21.4 degrees, 22.2 degrees and 26.3 degrees to 21.9 degrees, 26.1 degrees and 26.3 degrees for BL2, BL4 and BL5, respectively. The principal strains suggest that it is the long-term principal tensile behaviour ε_1 that has the greatest influence on the global deformation and that the compressive creep ε_2 played a smaller role. Even though the percentage increase of the principal compressive strain was greater than that of the principal tensile strain, for the observed principal directions, an increase in principal tensile strain led to a larger increase in transverse strain ε_y. Thus it follows that the time-dependent tensile behaviour of the reinforced concrete was the more dominant factor in the transverse strain increase in the shear links and CFRP straps.

Bending deflection

The global deflections obtained using the dial gauges are plotted in Fig. 11. The mean shear deformation of each rectangular element was calculated from equation (1) and, for the purposes of comparison, linear interpolation and extrapolation was used through the shear span to calculate the corresponding shear components of deflection at the locations of the dial gauges. These shear deformations were then deducted from the measured global deflections to isolate the time-dependent bending deflections. Across the five beams, the mid-span global deflections increased by between 79% and 101% whereas the mid-span bending components of deflection showed a somewhat lower increase of between 53% and 89%.

It is notable that the bending deflection components in BL1 were not as symmetrical as the global deflections. The bending deflections were influenced by the shear deflections, which contradicts the common assumption that the shear behaviour does not affect the bending

behaviour. For the left span of BL1, the dominant shear crack was significant and extended from the support to the loading point (see Fig. 5). Therefore the bending deflections were not evenly distributed along the shear span. In contrast, the bending deflections in the strengthened beams were relatively consistent in both shear spans.

The greater absolute level of sustained load in the strengthened beam BL2 (72 kN) led to greater initial bending deflections as well as a higher increase over time than in the unstrengthened beam BL1 which had a sustained load of 38 kN. The higher percentage increase (66%) in the bending deflection of BL2 can be partially attributed to the high-stress creep effects (CEB-FIP Model Code 2010, 2012). The creep deformation tends to develop more significantly when the stress in the compression zone is higher and the concrete behaves non-linearly. The percentage increase in bending deflection for strengthened beam BL4 with a sustained load of 50 kN was 62% and hence lay between that of BL1 (38 kN) and BL2 (72 kN). By comparing BL3 with BL2 it appears that the use of higher strength concrete in BL3 reduced the initial bending deflection as well as the subsequent increase even when BL3 was subjected to a higher sustained load in an absolute sense. This is due to the fact that the creep behaviour is lower when the concrete strength is higher. The sustained load level in BL5 (83 kN) was greater than that in BL2 (72 kN), however the initial bending deflections of BL5 were slightly less than those of BL2. Although the two beams had the same target concrete strength of 30 MPa, in practice, BL5 had a higher measured concrete strength (32.23 MPa) than BL2 (26.02 MPa). Over the long-term the bending deflections of BL5 exceeded those in BL2. This behaviour indicated that over the long term, the higher sustained load in BL5 was a more dominant factor than the difference in concrete strength.

Interaction of shear and bending deflections

In each beam, the time-dependent shear component of deflection at mid-span was isolated and the resulting percentage shear contribution to the global deflection is shown in Fig. 12. The

long-term shear proportion in the un-strengthened control specimen BL1 was greatest at around 42%. The CFRP straps were effective in reducing the proportion of the shear deflection even when in an absolute sense the sustained loads on the strengthened beams were higher. However, the shear proportions still represented 24% to 28% of the mid-span deflection over the long term, which was not negligible.

Future work and further considerations

In strengthened beams subjected to sustained loads, the shear deflections and strap strains increased with time and these phenomena should be reflected in design guidance to meet long-term serviceability and strength enhancement requirements. Time-dependent influences due to unbonded strap size effects whereby the strap force induced by a given crack opening is smaller for a deeper beam also require further investigation.

Any strengthening intervention is disruptive but strengthening can be the preferred option when compared with the alternatives such as load limits or structural replacement. The practical implications depend on the application e.g. research to explore the installation of CFRP straps using an underslab installation technique has been conducted (Hoult & Lees (2009)) and, as with any FRP strengthening system, the required fire performance and resistance need to be assessed. In the current work, the levels of sustained loads were relatively high such that the behaviour of the concrete, steel and CFRP straps after dominant shear cracks had formed could be interrogated. The actual in-service load conditions and any associated structural repairs will influence the load sharing and the long-term demands on the materials.

Conclusions

The unbonded pre-stressed CFRP strap shear strengthening technique provided an effective strength enhancement to reinforced concrete beams subjected to significant sustained loads for

a period close to a year. However, a certain allowance should be made to accommodate time-dependent increases in the strap strains. The main conclusions were:

(1) None of the CFRP-strap strengthened experimental beams collapsed after being subjected to significant sustained loads (greater than the unstrengthened static failure load) for approximately 320 days. This indicated that a properly designed CFRP strap strengthening system holds promise over the long term.

(2) The presence of the CFRP straps resulted in more smeared and uniform crack patterns. No new continuous shear cracks appeared during the tests. The crack opening (width and slip) magnitudes all increased over the long term. However, compared with the un-strengthened control beam, the magnitude of the increase was more limited in a strengthened beam. In the cracked shear spans, the maximum crack width and slip did not necessarily occur at the same location.

(3) Even though they were symmetric, the shear links in the two shear spans behaved differently. The differences over the long term depended on the magnitude of the initial strain. Some shear links did not yield initially but did so over the long term. However, by the end of the test duration, none of the shear links had failed.

(4) The CFRP straps need to be carefully designed to include the effects of long-term loading. The strains in the CFRP straps increased with time and the percentage increases (excluding the pre-strain) ranged from 3% to 42%. None of the straps ruptured in the long-term tests but the highest total strap strain developed in the specimen with a higher initial pre-stress and reached a strain magnitude where some damage to the straps could be expected.

(5) The extent of the time-dependent shear deformation, shear link strains and strap strains was primarily attributed to the principal tensile deformation.

(6) After 320 days, the initial global mid-span deflections had increased by between 79% and 101% from those measured on initial loading. The mid-span bending deflection components

increased by between 53% and 89% over the same period. The percentage increase in bending deflection was negatively correlated with the concrete strength. A high-stress creep effect due to a greater sustained load seemed to lead to greater creep deformations.

(7) The shear strains increased by between 156% and 242% , which were significantly greater as percentages than the bending deflection increases. The increase in the percentage of shear strain was negatively correlated with the concrete strength, not significantly affected by the magnitude of the external sustained load and reduced through the use of CFRP straps with a higher pre-stress. The shear deflection as a proportion of the global deflection increased over the long term and represented between 24% to 42% of the total deflection.

Acknowledgements

The authors would like to acknowledge the financial support of Cambridge Commonwealth and Overseas Trusts, the University of Cambridge Department of Engineering and Homerton College in the University of Cambridge. They are also grateful to Empa for their ongoing support.

References

Burgoyne, C. and Balafas, I., (2007). “Why is FRP not a financial success?” In *Proc. 8th Intl. Conf. on FRP Reinforcement for Reinforced Concrete Structures, FRPRCS-8*, Univ. of Patras, Patras, Greece.

CEB-FIP. CEB-FIP Model Code 2010-Final draft, (2012). Comité Euro-International du Béton, vol. 1.

Czaderski, C., Motavalli, M. and Winistoerfer, A., (2008). “Prestressed shear strengthening of a box girder bridge with nonlaminated CFRP straps.” Fourth International Conference on FRP Composites in Civil Engineering (CICE2008)

22-24 July 2008, Zurich, Switzerland.

De Lorenzis, L. and Nanni, A., (2001). "Shear strengthening of reinforced concrete beams with near-surface mounted fiber-reinforced polymer rods." *ACI Structural Journal*, 98(1), 60-68.

Dirar, S., Lees, J.M. and Morley, C.T., (2013). "Pre-cracked reinforced concrete T-beams repaired in shear with pre-stressed carbon fiber-reinforced polymer straps." *ACI Structural Journal*, 110(5), 855-866.

El-Hacha, R., Wight, R.G. and Green, M.F., (2003). "Innovative system for pre-stressing fiber-reinforced polymer sheets." *Structural Journal*, 100(3), 305-313.

Foster, R.M., Haria, S., Morley, C.T. and Lees, J.M. (2017) "Shear Capacity of Reinforced Concrete Subjected to Tension: Experimental Results and Analysis", *J. Struct. Eng.*, 143(9), 04017085.

Foster, R.M., Morley, C.T. and Lees, J.M. (2015) "Modified Push-Off Testing of an Inclined Shear Plane in Reinforced Concrete Strengthened with CFRP Fabric", *ASCE Journal of Composites for Construction*, 04015061.

Hoult, N.A., (2005). *Retrofitting of Reinforced Concrete Beams with CFRP Straps to Enhance Shear Capacity*, PhD Thesis, Department of Engineering, University of Cambridge.

Hoult, N.A. and Lees, J.M., (2009). "Efficient CFRP strap configurations for the shear strengthening of reinforced concrete T-beams." *Journal of Composites for Construction*, 13(1), 45-52.

Hoult, N. A., and Lees, J. M., (2011). "Time-dependent behavior of RC beams retrofitted with CFRP straps." *Journal of Composites for Construction*, 15(1), 75-84.

Jin, F. (2016). *Time-Dependent Behaviour of RC Beams Strengthened with Pre-stressed CFRP Straps*, PhD Thesis, Department of Engineering, University of Cambridge.

Kesse, G. and Lees, J.M., (2007). "Experimental behavior of reinforced concrete beams strengthened with pre-stressed CFRP shear straps." *Journal of Composites for Construction*, 11(4), 375-383.

Koppitz, R., Kenel, A. and Keller, T. (2014) “Effect of punching shear on load–deformation behavior of flat slabs” *Engineering Structures* 80, 444–457.

Lees, J.M. and Burgoyne, C.J., (1999). “Experimental study of influence of bond on flexural behavior of concrete beams pre-tensioned with aramid fiber reinforced plastics.” *ACI Structural Journal*, 96, 377-385.

Lees, J. M., Winistoerfer, A. U., and Meier, U., (2002). “External pre-stressed carbon fiber-reinforced polymer straps for shear enhancement of concrete.” *ASCE Journal of Composites for Construction*, 6(4), 249-256.

Lees, J.M. and Winistörfer, A.U., (2010). “Non-laminated FRP strap elements for reinforced concrete, timber, and masonry applications.” *Journal of Composites for Construction*, 15(2), 146-155.

Lima, J.L., and Barros, A.B. (2011) “Reliability analysis of shear strengthening externally bonded FRP models.” *Struct. Build.*, 64(1), 43–56

Meier, U. and Kaiser, H., (1991). “Strengthening of structures with CFRP laminates.” In *Advanced Composites Materials in Civil Engineering Structures*: 224-232. ASCE.

Motavalli, M., Czaderski, C. and Pfyl-Lang, K. (2010). “Prestressed CFRP for strengthening of reinforced concrete structures: Recent developments at Empa, Switzerland” *Journal of Composites for Construction*, 15(2), 194-205.

Stenger, F., (2001). *Tragverhalten von stahlbetonscheiben mit vorgespannter externer kohlenstofffaser-schubbewehrung* [Load-carrying behavior of reinforced concrete deep beams with external carbon fiber shear reinforcement]. Diss. ETH No. 13991, Institut für Baustatik und Konstruktion, ETH, Zürich, 153 (in German).

Teng, J.G., Chen, J.F., Smith, S.T. and Lam, L., (2002). “FRP: strengthened RC structures.” *Frontiers in Physics*, 266.

Teng, J. G., Chen, J. F., Smith, S. T., and Lam, L. (2003). “Behaviour and strength of FRP-

strengthened RC structures: A state-of-the-art review." *Proceedings of the ICE-Structures and Buildings*, 156(1), 51-62.

Triantafillou, T.C., (1998). "Shear strengthening of reinforced concrete beams using epoxy-bonded FRP composites." *ACI Structural Journal*, 95(2), 107-115.

Winistöerfer, A. U. (1999). *Development of Non-Laminated Advanced Composite Straps for Civil Engineering Applications*, PhD Thesis, University of Warwick, U.K.

Yapa, H.D. and Lees, J.M. (2013). "Rectangular reinforced concrete beams strengthened with CFRP straps." *Journal of Composites for Construction*, 18(1), 04013032.

Table 1 Experimental beams and test parameters

Specimen	f_{cu} (MPa)	Number of straps in shear span	Strap pre-stress (%)	Sustained load (kN)	Duration of sustained load (days)
BL1/C30/nS/S75	27.83	0	-	38	320
BL2/C30/P25/S75	26.02	2	25	72	320
BL3/C50/P25/S75	45.65	2	25	85	320
BL4/C30/P25/S50	25.54	2	25	50	321
BL5/C30/P50/S75	32.23	2	50	83	314

Table 2 Concrete mix (per m^3)

Target strength (MPa)	Cement (kg)	Water (kg)	Fine aggregate (0-2mm) (kg)	Coarse aggregate (0-10mm) (kg)
30	375	225	754	921
50	375	150	788	963

Table 3 Steel reinforcement properties

Bar type	Diameter (mm)	Yield stress (MPa)	Ultimate stress (MPa)
Smooth	4	475	514
Ribbed	8	520	620
Ribbed	16	509	609

Fig. 1. Shear strengthening using pre-stressed un-bonded CFRP straps

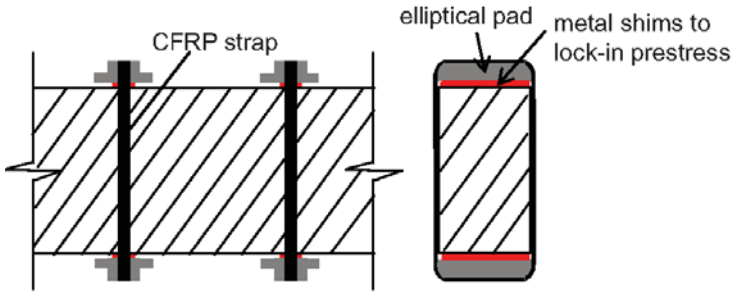

Fig. 2. Reinforcement layout in (a) cross-section and (b) unstrengthened and (c) strengthened RC beams

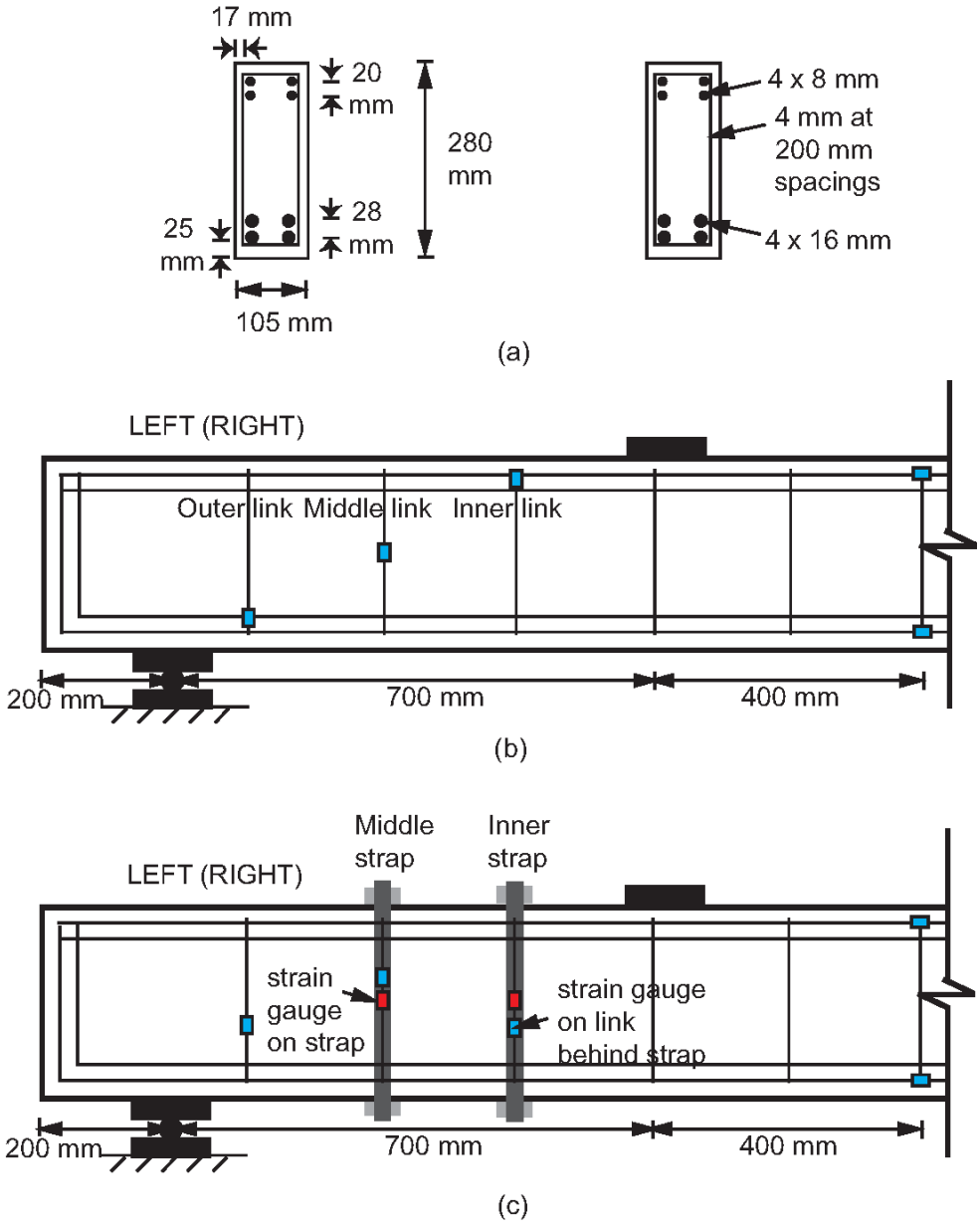

Fig. 3. Measurement scheme for long-term specimens (a) layout of measurement gauges (b) notation used for demec square element and (c) rhomboidal element crossed by a crack

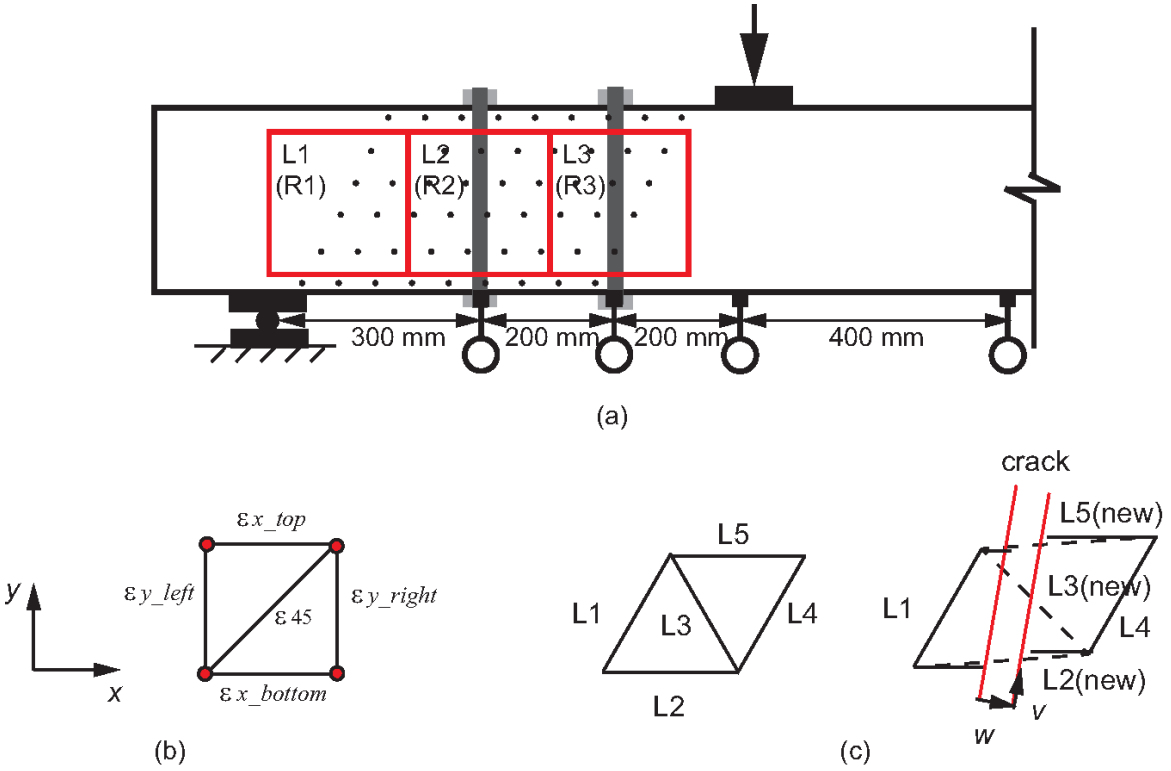

Fig. 4. Photo of test rig for long-term specimens

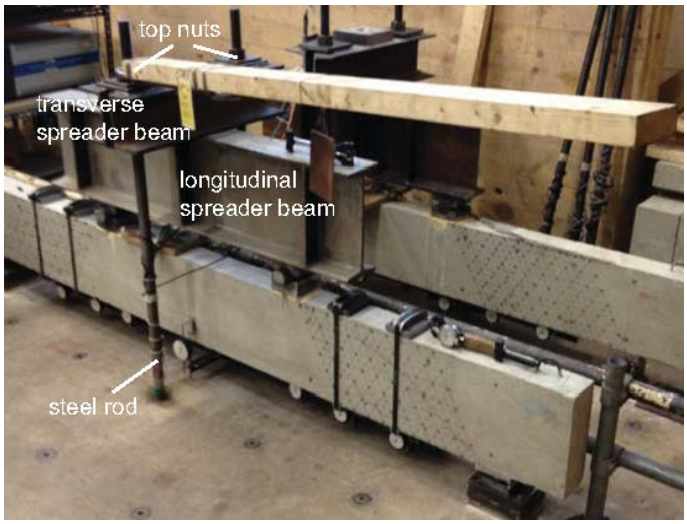

Fig. 5. Shear crack patterns (a) BL1(L) (b) BL1(R) (c) BL2(L) (d) BL2(R) (e) BL3(L) (f) BL3(R) (g) BL4(L) (h) BL4(R) (i) BL5(L) (j) BL5(R)

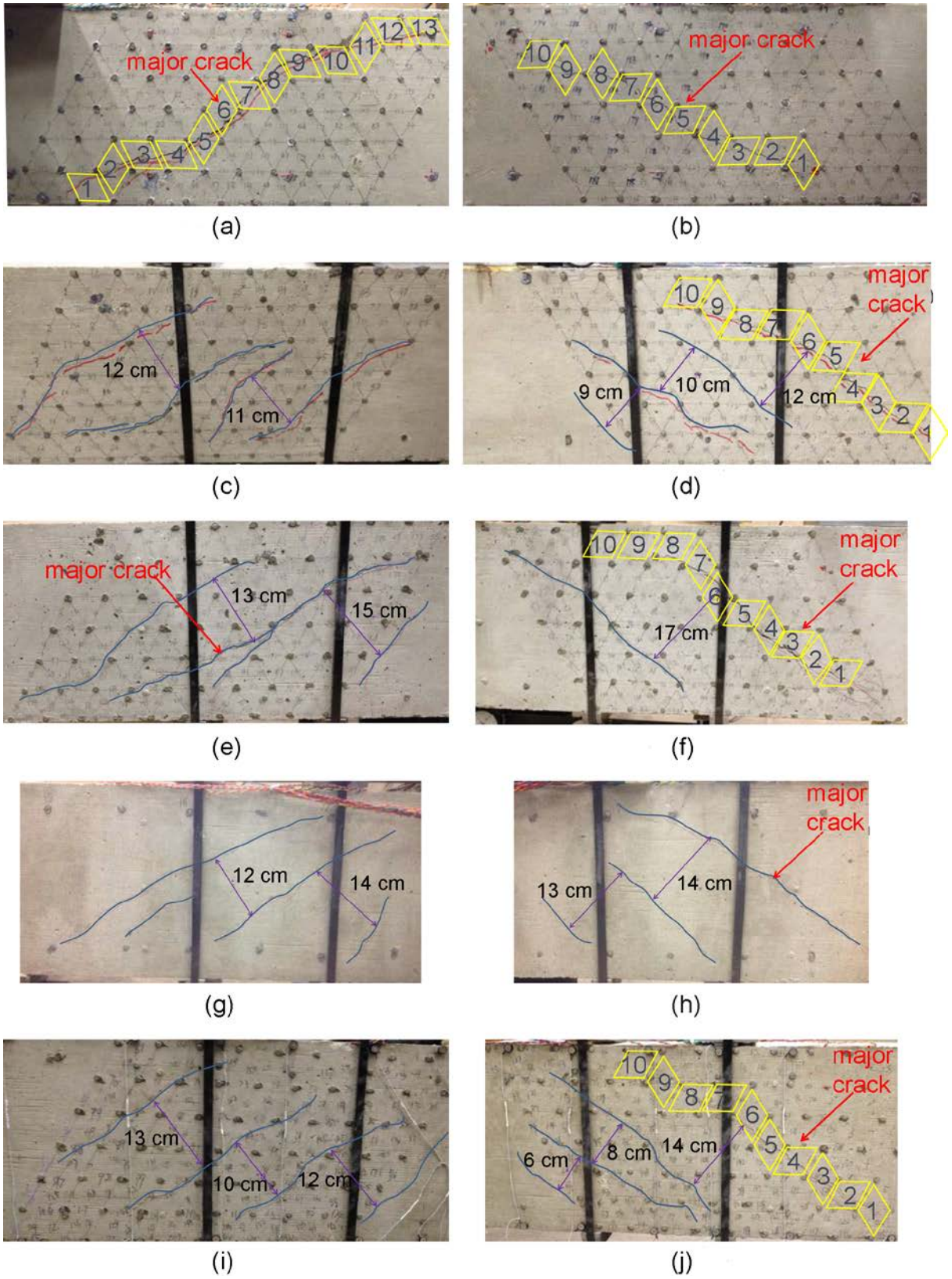

Fig. 6. Development of shear crack kinematics in (a) BL1 (L) (B) BL1 (R) (c) BL2 (R) (d) BL3 (R) and (e) BL5(R)

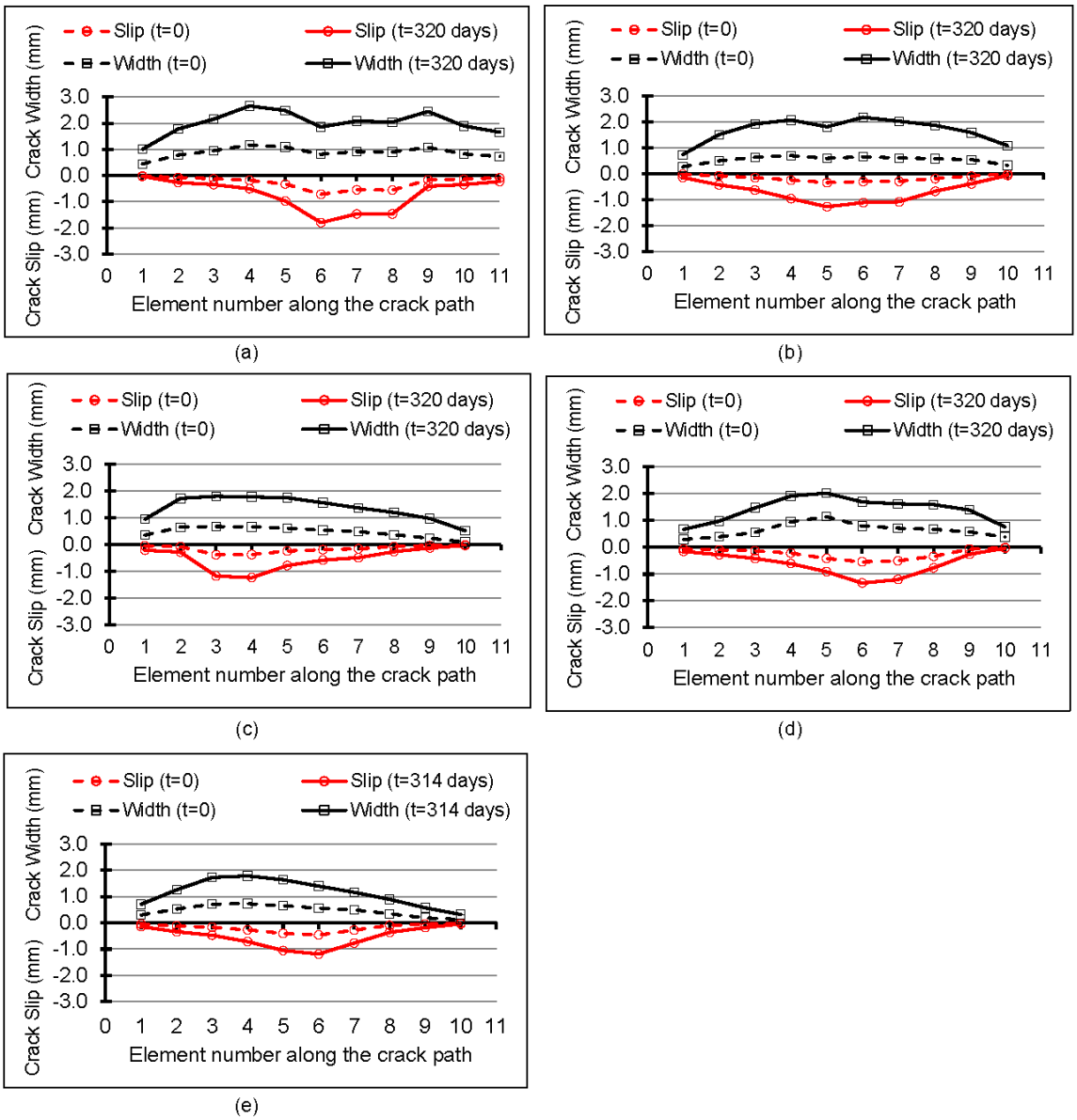

Fig. 7. Shear link strains (a) outer link (L) (b) outer link (R) (c) middle link (L) (d) middle link (R) (e) inner link (L) and (f) inner link (R)

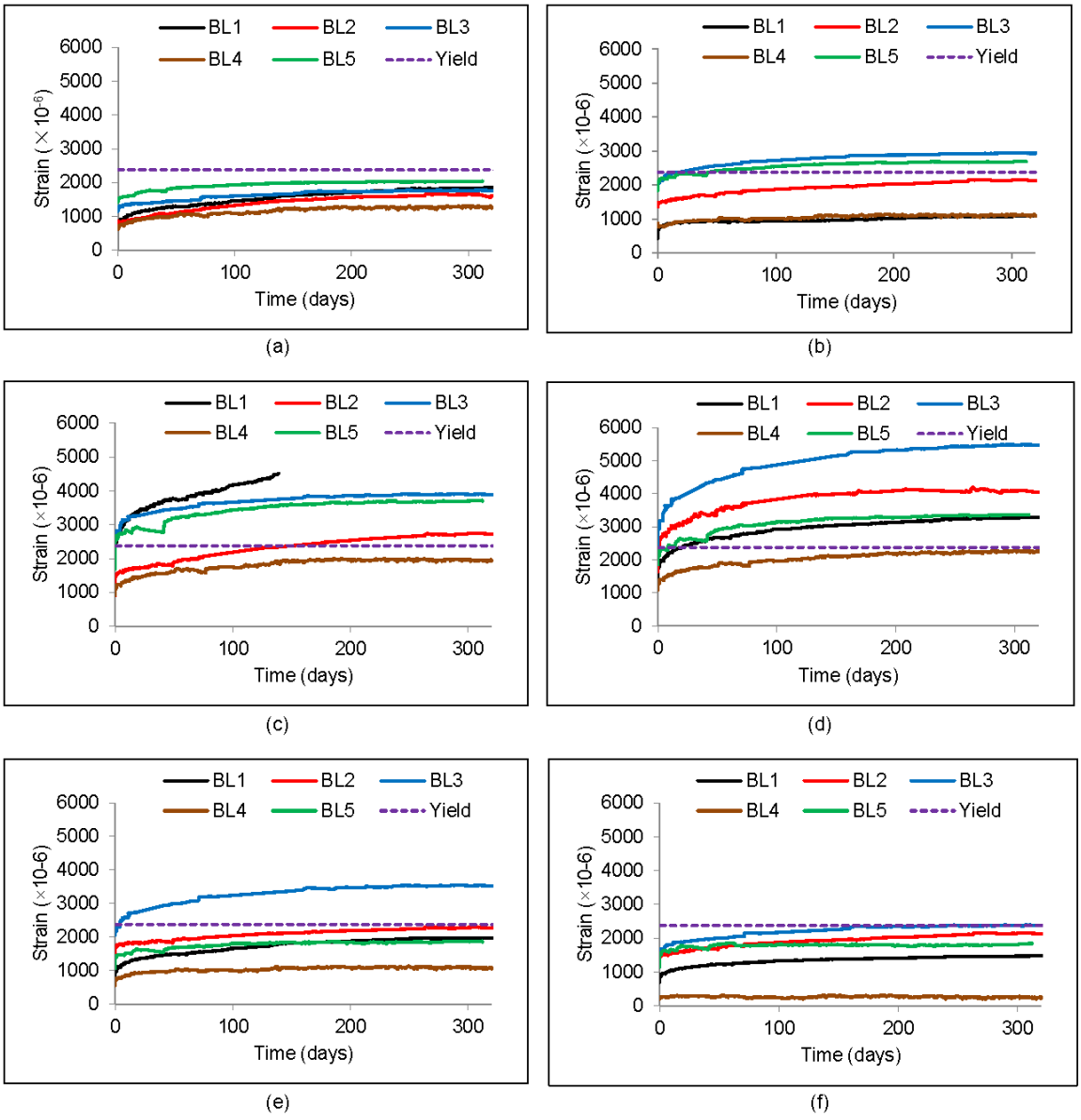

Fig. 8. Strap strains in long-term specimens (a) BL2 (b) BL3 (c) BL4 and (d) BL5

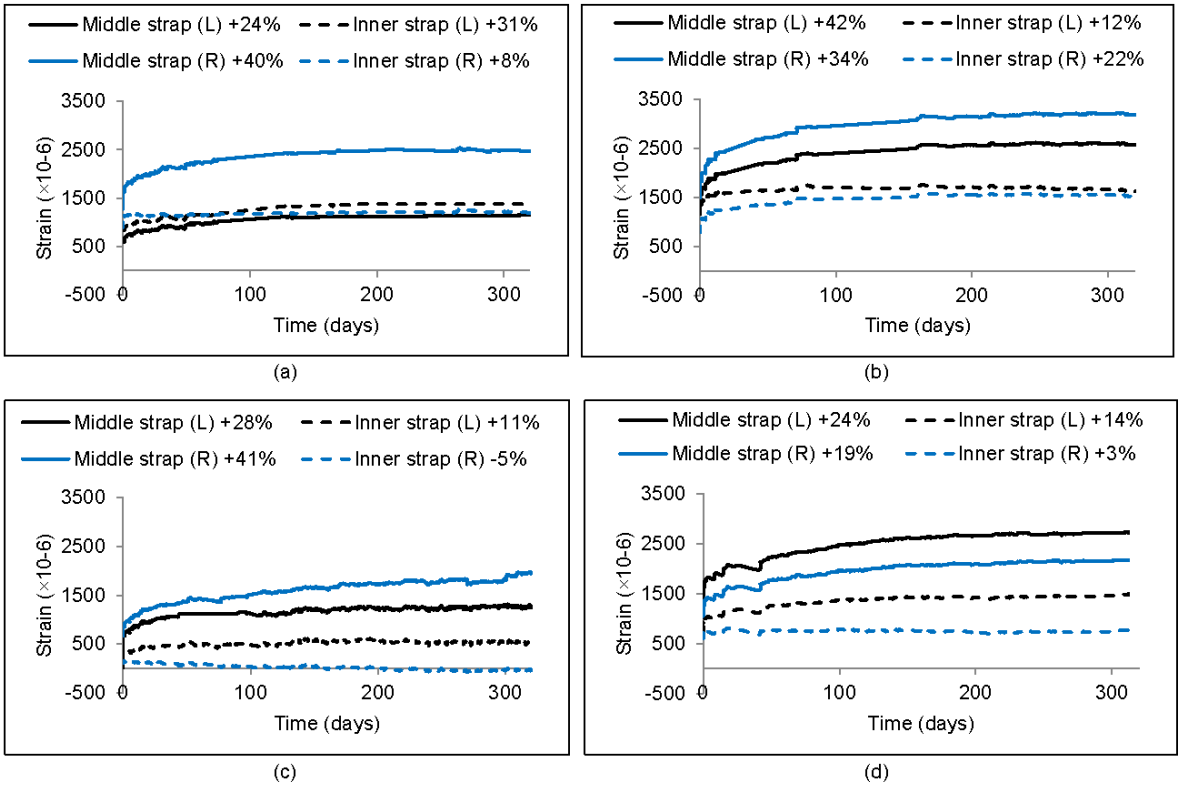

Fig. 9. Mean shear strain in the (a) left and (b) right, shear spans of the long-term specimens

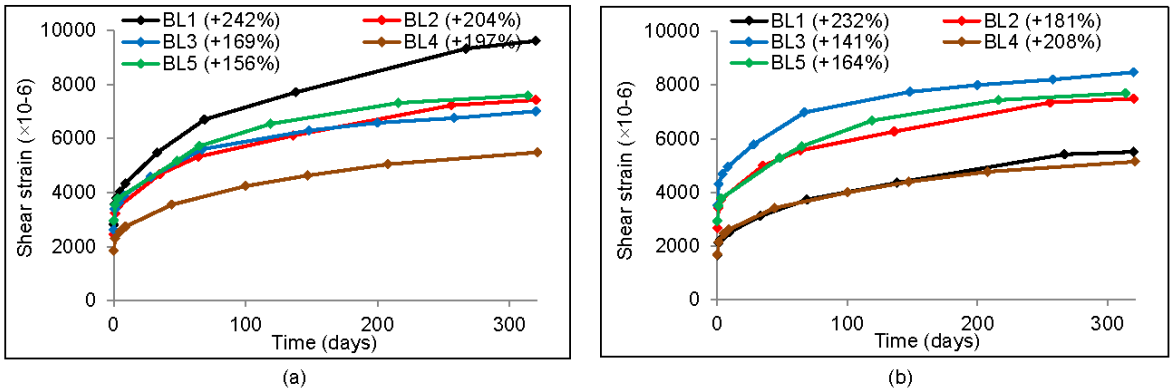

Fig.10. Mohr's circle of strain for element R2 in (a) BL2 (b) BL4 and (c) BL5

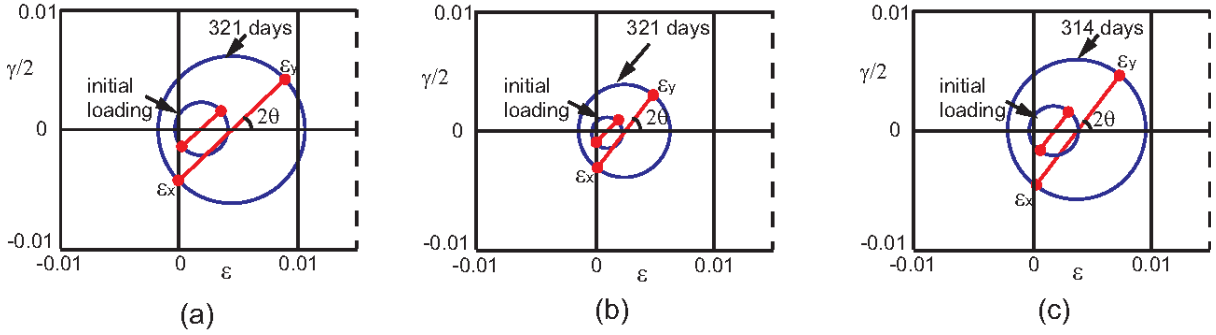

Fig. 11. Beam deflections over the long term (a) BL1 (b) BL2 (c) BL3 (d) BL4 and (e) BL5

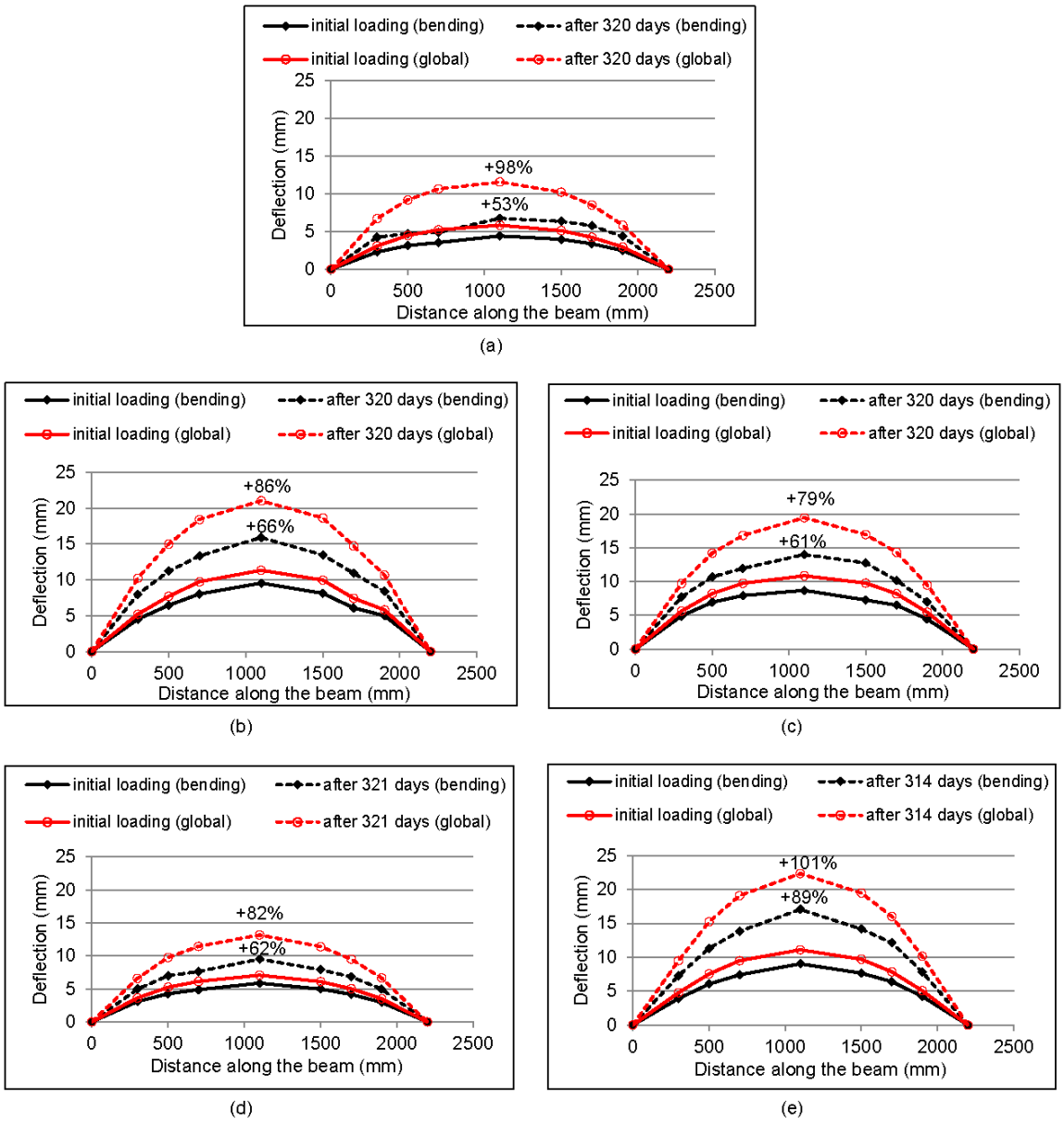

Fig. 12. Shear deflection proportions at mid-span